Wavebased Micromotor for Plane Motions (3-DoF)

Georg Jehle[1], Dominik Kern[1,*] and Wolfgang Seemann[1]
[1]Chair for Engineering Mechanics (ITM), Karlsruhe Institute of Technology (KIT), Germany
*Corresponding author: KIT Campus Süd, Kaiserstraße 10, kern@kit.edu

Abstract: This paper proposes the design of a 3-Degree of Freedom (DoF) motor for plane motions based on surface acoustic waves (SAW) in elastic solids. The rotor is propelled by wave fields in the stator that can be steered by the driving signal of the piezoelectric actuators, which are placed on an elastic plate. The feasibility of the motor is demonstrated by the means of simplified analytic models. The simulation results are obtained by a FEM-model, which was iteratively built as the first attempts suffered certain deficiencies, technically as well as numerically. The paper closes with an outlook to future modifications of the motor, inspired by observations made in the simulations.

Keywords: ultrasonic motor, wave propagation, piezoelectric actuators, MEMS

1. Introduction

The travelling-wave type motor as proposed by Sashida [1] found its way into versatile applications in mechatronic and microelectromechanical systems (MEMS). Wave based motors are striking for their advantages: high positioning resolution, compact size, large power density, high torque at low speed, high stationary limiting torque when switched off and absence of electromagnetic radiation. Furthermore, no lubrication is needed, which predestines these motors for applications under vacuum atmosphere.
Rotational motors and linear motors are state of the art. Rotational ultrasonic motors are widespread in the industry, for instance as ultrasonic lens motors in the photo cameras of the Canon USM series, while linear motors are subject of research yet. Promising experimental investigations were reported, e.g. by Feenstra [2]. The success of the existing rotational ultrasonic motors and the development of linear ultrasonic motors inspired this work about a 3-DoF motor. The idea is to generate wave fields that move the rotor along a two-dimensional trajectory and rotate it in order to obtain a general motion in the plane. Particular advantageous is the rotor positioning in x- and y-direction and rotating simultaneously, avoiding position error accumulation, as it happens for sequential placement of conventional kinematics.

The application of steered waves in elastic solids is not bounded to the present motor. Besides, there are innovative ideas for miscellaneous applications. For instance, as high frequent oscillation reduces the friction force and acts as liquid-free microlubrication [7], the friction between a stator and contacting objects can be actively controlled not only in value but also in directivity. This results in an anisotropic friction coefficient, which might be interesting for sorting processes of granular media. Also fluid flows in the boundary layer around a solid could be biased by acoustic surface waves. Extending this idea to the transport of fluids might result in an active gasket, where the waves actively prevent the fluid from leaking.
Another application is developing in the field of structural health monitoring (SHM), where steered waves scan a structure in a radar-like fashion in order to detect damages [5].

The next words give an outline about this article. At first the feasibility of the motor is substantiated by two simple analytic models, one for the friction based transport mechanism and one for the wave steering. From these considerations follows the construction of the motor, which is the physical model for the simulations. The main section is devoted to the numerical model, the governing equations and their solution by FEM. These simulations fully utilize the possibilities of today's numerical computing as they account for the transient solution of waves generated by an array of piezoelectric actuators and the dynamic contact between rotor and stator. The results not only gave rise for modifications of the construction but also inspired new ideas, which conclude this paper.

2. Preliminary Considerations

The two basic mechanisms underlying the motor are the friction based propulsion force produced

by the rotor-stator contact and the steerable wave field in the stator. The basic model for the rotor-stator contact is derived from the theory of tribological contacts. The strategy for the steered wave fields originates from the antenna theory for electromagnetic waves.

2.1 Rotor-Stator Contact

The proposed motor is of the travelling wave type, the transport is powered by the friction between rotor and the stator surface points, which move along an elliptic trajectory. Several models for the rotor-stator interaction are listed in the review by Wallascheck [3] about contact mechanics of piezoelectric ultrasonic motors. One of the simplest models is a line contact with stiffness in normal direction only, as illustrated in fig. 1.

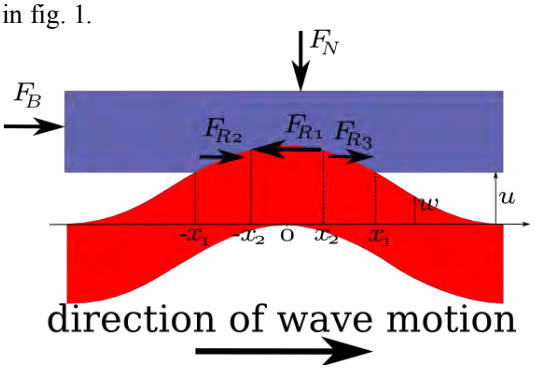

Figure 1. The rotor-stator contact is modeled as line contact between a rigid stator, whose deformation follows exactly the prescribed wave motion, and a rotor, which is elastic in normal direction only.

The tangential velocity of the stator surface points is a spatially and time varying function with maxima at the wave crests (top) and minima at the wave troughs (bottom). The rotor velocity is between these minima and maxima. It can be at most as high as the tangential velocity at the wave crests. Thus there are segments with negative and positive relative velocity, depending on the length of a contact and the rotor velocity. At the positions $-\boldsymbol{x_2}$ and $\boldsymbol{x_2}$ the relative velocity vanishes. In between the friction force $\boldsymbol{F_{R1}}$ has the desired direction, whereas in the outer segments the friction force is in the opposite direction. Integrating the friction force over the contact length results in a propulsion force. The motor characteristics speed versus propulsion force for different values of the normal force are shown in fig. 2.

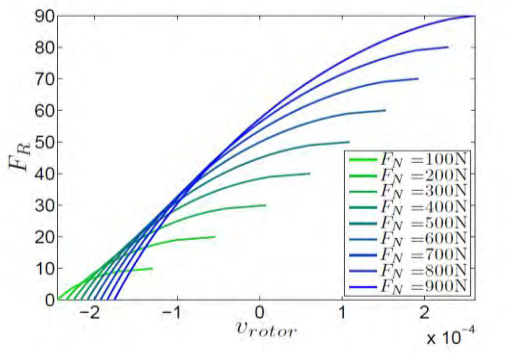

Figure 2. The motor characteristics driving force F_R vs. rotor speed v_{rotor} for several values of the normal force F_N. The line ends when the rotor starts sliding, i.e. the transport fails.

In order to decrease the repulsion in vertical direction during the contact between rotor and stator, rigid contact surfaces are not very suitable. On the other hand, the rotor should be relatively stiff so that the normal force is constant in all contact points. Therefore, the rotor is separated into two parts: A soft contact layer and an element with a high stiffness on top as can be seen in the sketch of the assembly in fig.5. The soft layer does not affect the dynamic properties of the whole system. It only improves the contact behavior.

We consider now an elastic wave that moves through the stator. For the kinematics of the wave motion, the coordinates of the surface points on the stator are of interest. From the coordinates, the trajectories can be derived easily by considering a fixed point and a variable time. As it can be seen in fig. 3, they are elliptic and have – independent from the coordinates – the same direction of rotation.

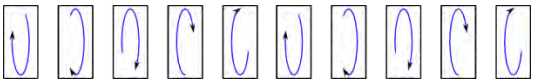

Figure 3. Trajectory of surface points at different positions (x-coordinate) of the stator while a wave passes.

The transport mechanism is based on this finding, because objects that lie on the surface of the waveguide are moved into the direction of rotation. The elliptic trajectories are only produced by traveling waves. Hence standing waves must be prevented, since they impair the transport mechanism.

2.2 Stator Wave Field

The focusing and steering of electromagnetic waves is widespread in telecommunications and radar applications. The underlying theory is described in many textbooks about antenna theory, e.g. in Balanis [4]. The adaption to elastic waves has been studied in the context of structural health monitoring, e.g. by Giurgiutiu [5]. Therefore the principles from active phased radar from antenna theory served as model. The direction-dependent amplitudes are expressed mathematically as group factor. Fig. 4 shows the group factor for several directions. One can see that wave fields with a governing main lobe and very little side lobes can be excited with an adequate steering, i.e. phase shifted excitation. The simulations were carried out for a general wave function. Although electromagnetic and mechanical waves are of different nature, they share a similar mathematical description. In the numerical simulations (paragraph 4), we will see, that mechanical waves are steerable with a high precision applying methods from the theory of electromagnetic waves.

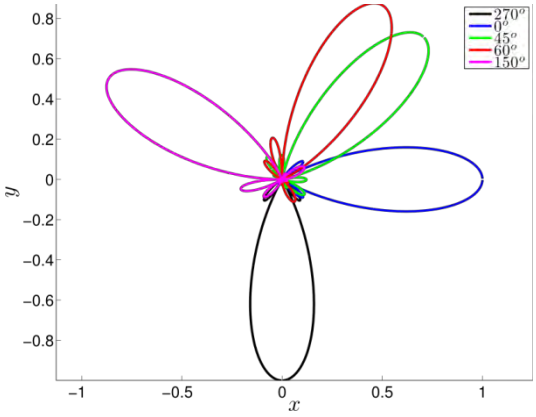

Figure 4. The group factor for the directions $0°, 45°, 60°, 150°, 270°$ of the main lobe.

3. Construction of the motor

The results of the preliminary considerations suggest further investigations. Fig. 5 illustrates schematically the construction of the motor. The stator is a plate made of an elastic material, e.g. a metallic alloy or synthetics.
The piezoelectric actuator arrays are placed in the fringe of the plate, around the operating area. They are either used as sources for generating the waves or as sinks for actively damping out the waves in order to minimize reflections.

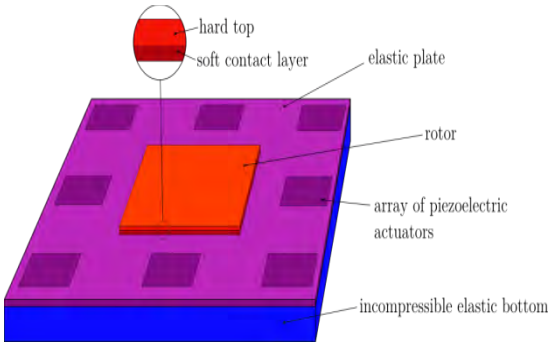

Figure 5. Schematic construction of the motor.

The motivation for the bedding of the plate in rubberlike, incompressible, low-density cushions as well as the soft contact layer of the motor arose during the numerical simulations.

4. Numerical Model

The transient analysis of FEM-models including rigid body modes and dynamic frictional contact is on the cutting edge. Moreover the combination with piezoelectric actuators needs the coupling of the application modes, namely a mechanical and an electrical.
This section formulates the mathematical model of the motor, the use of COMSOL Multiphysics for the numerical solution and the iterative modifications of the constructions leading to the final design.

4.1 Governing Equations

The governing equations for the mechanical fields are from the linear theory of elasticity. The variable $\boldsymbol{u}$ denotes displacement vector, $\boldsymbol{b}$ the body force vector, while μ and λ represent Lame's constants and ρ density.

$$\rho \boldsymbol{u}_{,tt} = \rho\, \mathbf{b} + \mu\, \nabla^2 \mathbf{u} + (\lambda + \mu)\mathrm{div}\big(\mathrm{grad}(\mathbf{u})\big) \tag{1}$$

The actuators constitutive equations are from the linear piezoelectricity and express the relation between mechanical strain ε and electric displacement D on the left hand side and mechanical stress σ and electrical field strength e on the right hand side coupled by the mechanical

compliance S, electromechanical coupling constant d and permittivity at zero mechanical stress ε^{σ}.

$$\varepsilon_{ij} = \sum_k \sum_l S_{ijkl}\, \sigma_{kl} + \sum_k d_{kij} e_k \quad (2a)$$
$$D_i = \sum_j \sum_k d_{ijk} \sigma_{jk} + \sum_j \varepsilon_{ij}^{\sigma}\, e_j \quad (2b)$$

The frictional contact is modeled as function of the ratio between normal and blocking force.

$$\left|\frac{F_N}{F_B}\right| \begin{cases} \leqq \mu_s \ , \ v_{rel} = 0 \\ = \mu_d + (\mu_s - \mu_d) e^{-c|v_{rel}|}, \ v_{rel} \neq 0 \end{cases} \quad (3)$$

The excitation of the wave is initiated by the electric field as dynamic boundary conditions. There were several models, plate models (Mindlin Plate) as well as continuum, build in 3D for the wave steering. The whole system with transport of the rotor was modeled in 2D only. This will be detailed in the next sections. The material data for the plate (structural steel) and the actuators (Barium Sodium Niobate) were taken from the material library. The bonding layer in between was assumed to have a Young's Modulus of $E = 3 \cdot 10^9$ Pa and a Poisson's Ratio of $\nu = 0.4$. The plate length and thickness are 1 m and 0.003m, respectively. The actuator diameter and thickness are 0.0116m and 0.001m. The bonding layer is assumed to be of 10^{-5}m thickness.

4.2 Wave Field in the Stator

Prerequisite for the 3DoF is a steerable wave field. The figures 6(a) and 6(b) show the wave field for a translation (angle: 80°) and for a rotation.

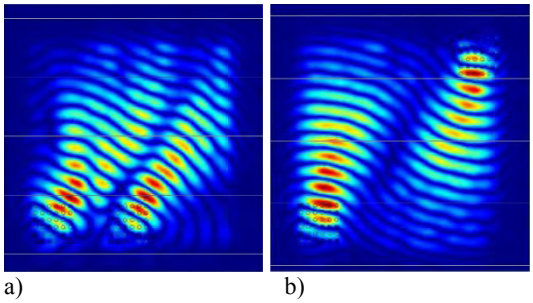

a) b)

Figure 6. Two exemplary simulations of the wave field in the stator (a) for a translation of the rotor (80°) and (b) for a rotation.

The laws from the antenna theory (section 2.2) were used for the driving signal of the actuators.
Damping at the edge is to prevent reflections. Since the active damping is not implemented yet a workaround utilizing the Rayleigh damping-model was made. In COMSOL, this was set in the "subdomain settings" dialogue box in the tab "damping", where a stepwise-constant law (step function σ) of the form

$$\alpha_D = \hat{\alpha}\sigma(x - x_0) \quad (4a)$$
$$\beta = 0 \quad (4b)$$

for the mass proportional damping coefficient α was implemented, while the stiffness proportional contribution β was set to zero. The coefficient $\alpha_D(x, y)$ was also defined coordinate dependent in order to increase the damping exponentially towards the fringe. The damped area, where the damping applies, is colored dark green and labeled "structural damping" in fig. 7.
Further settings were given through the predefined Multiphysics coupling "Piezo-Structural Interaction" in 3D with a transient analysis.

4.3 Simulations of the Transport

The prescribed wave motion works for the transport of objects. In this section, the simulation of the transport mechanism with COMSOL is described.
As before, the model is built in the "Piezo-Structural Interaction" application mode, but this time in 2D. Because of the non-linearity, the dynamic contact between stator and rotor requires an extra attention.
After defining contact edges (master & slave), in the B.C.-dialogue box the friction law and the penalty factors can be set. For an exact simulation, these factors should be high enough, but if they are too high the convergence rate becomes extremely bad. Additionally, in the "Solver Settings" dialogue box the tolerances and the estimated values for all quantities can be set - in the case of dynamic contacts, this is essentially for the requisition of a solution.
Despite these settings, the results of the model were not as initially expected and so stepwise refinements were made to improve the solution quality.

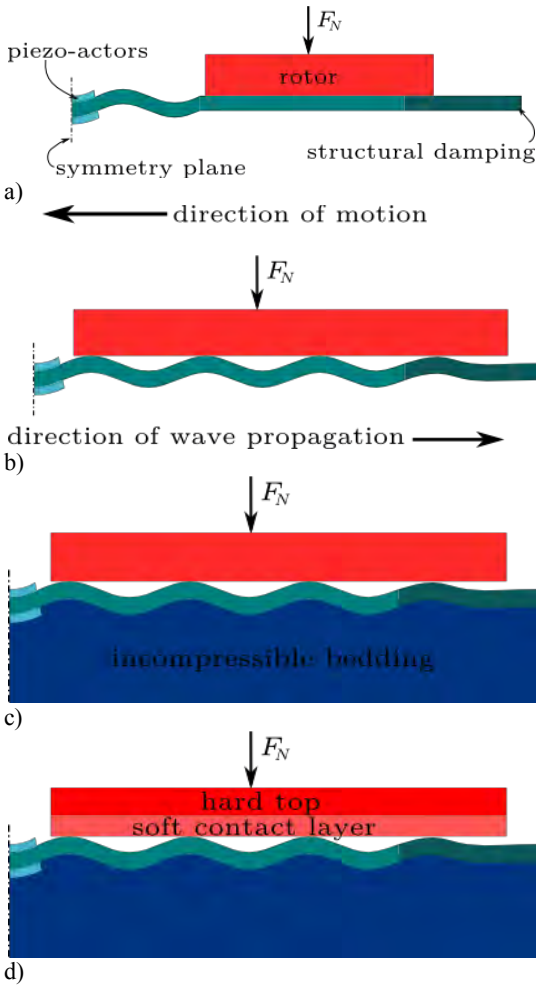

Figure 7. Stepwise modifications of the motor (a) original model, (b) adapted initial conditions, (c) incompressible bedding to prevent static deflection, (d) soft contact layer to prevent repulsion of the rotor.

For a high stability of the simulation, initial conditions such that the first contact is not a too big bound should be implemented. To set an initial contact between rotor and stator and an initial wave speed turned out very useful in this model.

The next problem is the static deflection of the stator which is induced by the rotor. The idea to prevent this effect is to use an incompressible cushion as described before.

After avoiding the deflection, the rotor is repulsed strongly by the first contact. Therefore, the rotor is separated in a soft contact layer and a rigid top. The stepwise refinements of the motor are illustrated in fig. 7.

A problem that could not be solved by a better model is the formation of additional waves in all contact points. In the COMSOL model, no travelling wave motion was observable after the reflections at the contact points occurred and resulted in standing waves. Thus further investigations were necessary in order to get an idea which parameter to tune for a better transport of the rotor.

These investigations were made with an analytical model of an Euler-Bernoulli-Beam and a singular deflection-proportional force acting orthogonal to the middle line. The results predict a higher transmission at lower normal forces and higher frequencies. The normal force is essential for a motor, so reducing it is not an option. Increasing the frequency requires a finer discretization of the model, which leads to a larger computational problem to be solved. Therefore, a full simulation of the system preventing the perturbing waves is not feasible on a desktop PC and persists to be done.

5. Conclusions

The FE-methods provided by COMSOL, which were used for the analysis of the wave-based motor, are capable of the complex models of transient wave propagation processes with contact and rigid body motion. However, they are computationally expensive. The use of parallelized computations on a high-performance cluster is considered for the future in order to run simulations of the complete motor from modeling every single piezoelectric actuator to the two-dimensional contact between rotor and stator. The frequencies of interest are above 1MHz, as reported from experiments [2]. Such parameters dictate a very fine meshing. Such simulations likely will give even more insight into the processes from the wave excitation to the transport, than the here presented ones, that were carried out on a Desktop PC.

So Instead of working with an all-in-one model, the aspects of wave beam forming and the contact mechanism were investigated separately with excitation frequencies in the range of 5 up to 40 kHz.

The steering of the wave field in the stator was analyzed with plate and continuum models. The generation of the wave field took into account the coupling between piezoelectric actuators with the plate, as they were modeled as

electromechanical system with the electrical boundary conditions (driving voltage).

The contact between stator, through which the wave passes, and the rotor was investigated in two dimensions. This model can be thought as a cross-section through the three dimensional model along the desired transport direction of the rotor.

These calculations led to useful indications for constructive modifications of the motor, such as the plate bedding, the contact layer and additional damping in the fringe.

As problem remained the reflection of waves at the contact with the rotor. However, if as assumed the reflections decrease with higher frequency, so that the transport mechanism does not deteriorate distinctly, a virtue can be made out of necessity. The reflections can be used for position detection. From the information contained in the reflections, the shape and the force distribution could be reconstructed. The piezoelectric actuator arrays allow the precise shaping of the wave field. Conversely this means, that their sensor signals provide extensive information about the sources of the reflections. The extraction of the sensor signal could be done by self-sensing circuits [6] resulting in a motor with integrated position detection. Figuratively expressed, this would incorporate some kind of mechanical touchscreen into the motor, which would be even interesting as a standalone application, if more attention is paid to the contact information than the transport.

At the current stage the proposed motor is a vision inspired by possibilities of today's technologies that appears feasible. It is important for further research to take into account economic facts such as costs, efficiency and future markets.

6. References

1. T. Sashida, A prototype ultrasonic motor – principles and experimental investigations, *Oyobutsuri (Applied Physics)*, **51**, 713-720 (1982)

2. P.J. Feenstra, P.C. Breedveld, J.v. Amerongen, *Actuation methods for a Surface Acoustic Wave Motor*, 2th International Workshop on Piezoelectric Materials and Applications in Actuators, Paderborn/Germany (2005)

3. J. Wallascheck, Contact mechanics of piezoelectric ultrasonic motors, *Smart materials and Structures*, **7**, 369-381 (1998)

4. C.A. Balanis, *Antenna Theory Analysis and Design*, 283-304, John Wiley (2005)

5. V. Giurgiutiu, L. Yu, In situ 2-D piezoelectric wafer active sensors arrays for guided wave damage detection, *Ultrasonics*, **48**, 117-134 (2007)

6. A. Preumont, *Mechatronics – dynamics of electromechanical and piezoelectric systems*, 185-191, Spinger (2006)

7. B. Bushan, *Tribology issues and opportunities in MEMS,* 463-469, Kluwer (1998)